Plant, Cell & Environment

WILEY

Plant, Cell & Environment

ORIGINAL ARTICLE

Correlation Analysis of Secondary Metabolism and Endophytic Fungal Assembles Provide Insights Into Screening Efficient Taxol-Related Fungal Elicitors

Mingshuang Wang | Xueshuang Liang | Ruoyun Ma | Wanting Lin | Zijin Fang | Lingxiao Zhang | Ganlin Chen | Jiaxu He | Enhui Bai | Erxu Pi | Pengcheng Zhang | Huizhong Wang | Chenjia Shen

College of Life and Environmental Sciences, Hangzhou Normal University, Hangzhou, China

Correspondence: Chenjia Shen (shencj@hznu.edu.cn)

Received: 11 September 2024 | **Revised:** 15 January 2025 | **Accepted:** 22 January 2025

Funding: This work was funded by the National Natural Science Foundation of China (Grant Nos. 32271905 and 32270382), the Zhejiang Provincial Natural Science Foundation of China (Grant Nos. LY23C160001 and LY22C020001), and Hangzhou Joint Fund of the Zhejiang Provincial Natural Science Foundation of China (Grant No. LHZY24C140001).

Keywords: correlation analysis | endophytic fungi | fungal elicitor | jasmonic acid | Taxus

ABSTRACT

The efficacy of Taxol, a natural anticancer drug, in the treatment of various types of cancers has been certified globally. Fungal elicitors have been reported as an impressive strategy for enhancing Taxol biosynthesis. We have investigated the effect of twig age on Taxol biosynthesis and the communities of endophytic fungi. A negative correlation between Taxol content and the complexity of the endophytic fungal community in twigs was predicted. Endogenous taxoids, similar to balancing valves, might have a specific effect on controlling the microbiota assembly in *Taxus* twigs. Utilising the special correlation, 11 isolates of twig age-associated fungi were used to screen new fungal elicitors involved in Taxol biosynthesis. Two efficient fungal elicitors, L01 (*Guignardia*) and J02 (*Diaporthe*), were identified, increasing the Taxol contents by 5.91- and 4.83-folds, respectively. It is confirmed that effective fungal elicitors may be negatively correlated with Taxol contents in *Taxus* tissues. Furthermore, the J02 and L01 fungal elicitors significantly induced the jasmonic acid (JA) content, speculating the involvement of MYC2a-controlled JA signalling in fungal elicitor-activated Taxol biosynthesis. Our data revealed the effect of twig age on Taxol biosynthesis of *Taxus* and provided a novel approach to screen effective fungal elicitors involved in Taxol biosynthesis.

1 | Introduction

Taxus species, which are rare and endangered woody species, have significant medicinal ingredients (Chunna Yu et al. 2021). Taxol was firstly extracted from the bark of the yew (*Taxus brevifolia*) and now can be detected in all species in the genus *Taxus* (Wani and Horwitz 2014). The efficacy of Taxol (trade name: paclitaxel) in the treatment of various cancers has been widely certified (Li et al. 2023). With the increasing demands, the supply of Taxol is in short (Xue et al. 2020). Therefore, it is extremely urgent to explore a cost-effective way to enhance the accumulation of Taxol and/or its intermediates in *Taxus* tissues (Yu et al. 2022).

So far, tremendous efforts have been made to reveal the Taxol biosynthesis pathway, consisting of nearly 30 steps (Kaspera and Croteau 2006; Zhan et al. 2023). Although the biosynthesis pathway of Taxol has been preliminarily elucidated, Taxol represents a formidable synthetic challenge (Zhang et al. 2023). Currently, the twigs of *Taxus* trees are the main sources for Taxol extraction. Increasing the Taxol yield in the twigs of

Mingshuang Wang and Xueshuang Liang contributed equally to this work.

Taxus trees is an effective way to address the supply and demand of Taxol (Exposito et al. 2009).

The induction and regulation of Taxol biosynthesis in *Taxus* tissues is a research hotspot. Due to the low and unstable levels of Taxol, several factors, such as methyl jasmonate (MeJA), salicylic acid (SA), coronatine (COR), polyethylene glycol (PEG), and cyclodextrin (CD), were applied to enhance Taxol biosynthesis in cultured *Taxus* cells or tissues (Demidova et al. 2023; Gallego et al. 2015; Zhao et al. 2023). For example, a mixture of MeJA solution elicited Taxol biosynthesis in *T. media* hairy root cultures by regulating the expression of *TS*, *BAPT*, and *DBTNBT* genes (Sykłowska-Baranek et al. 2022). Treating *T. media* cell cultures with the elicitor COR enhanced the taxane production by 15-fold compared to the control (Escrich et al. 2021). Several salicylic acid (SA) responsive transcription factors (TFs) regulate the expression of most Taxol biosynthesis genes, suggesting that SA is also an effective chemical elicitor involved in Taxol biosynthesis (Y. Chen et al. 2021). However, chemical reagents frequently cause secondary pollution, which affects the quality of Taxol extracts, significantly limiting the application of chemical elicitors.

A number of endophytes exist in the intercellular space of medicinal plants, including *Taxus* trees (Zhang et al. 2024; Zhang et al. 2024). Many endophytic fungi have been reported to be involved in activating plant secondary metabolism. Several geographically associated endophytic fungi play important roles in the accumulation of tropane alkaloids in *Anisodus tanguticus* (Wang et al. 2023). Introduction of *S. indica* led to a substantial rise in the contents of flavonoids and phenols in the leaves and seeds of Tartary buckwheat (Zheng et al. 2023). Two endophytic fungi, *Penicillium canescens* and *Talaromyces*, have beneficial effects on tanshinones and phenolic compounds of *Salvia abrotanoides* (Masoudi Khorasani et al. 2023). Moreover, three endophytes isolated from the rhizomes of *Houttuynia cordata*, including *Ilyonectria liriodendra*, unidentified fungal, and *Penicillium citrinum*, increased the accumulation of phenolics and volatiles, as well as several medicinal compounds (afzelin, decanal, 2-undecanone, and borneol) (Ye et al. 2021).

Interestingly, several endophytic fungi of *Taxus* trees have been reported to act as elicitors in Taxol production. Application of *Aspergillus niger*, an endophytic fungus found in the inner bark of *T. chinensis*, resulted in a great increase in Taxol biosynthesis (Wang et al. 2001). Treatment with fungal elicitors significantly increased Taxol biosynthesis in the cell culture of *Corylus avellana* (Salehi et al. 2020). An endophytic fungus KL27 significantly promoted the level of Taxol in the needles of *T. chinensis* by regulating the expression of several key genes involved in the upstream pathway of terpene synthesis (Cao et al. 2022). Screening for more efficient fungal elicitors can increase the yield of Taxol in an environmentally friendly way.

The distribution of endophytic fungi in plant tissues exhibits spatiotemporal variation. Previous studies have shown that the hosts' age significantly affects the occurrence of endophytes in the rhizosphere of *Ginkgo biloba* (Kumar, Singh, and Pandey 2009). High-throughput sequencing illustrated the variation in endophytic fungi of tea plants with different ages (Wu et al. 2020). The fungal microbial communities associated with different medicinal plants, such as *Rheum palmatum* and *Paris polyphylla*, were also affected by the host's ages (D. Chen et al. 2022; Liu, Greenslade, and Yang 2017). In the present study, we investigated the effect of twig age on the secondary metabolism of *T. mairei* and identified several endophytic fungi related to Taxol biosynthesis. Two efficient fungal elicitors for the enhancement of Taxol biosynthesis also have been isolated, revealing a new approach to regulating the biosynthesis of Taxol.

2 | Results

2.1 | Variations in Metabolic Profiling Among Twigs With Different Ages

The twigs of the *Taxus* tree are the primary resources for extracting Taxol. Five twig samples with different ages were harvested from the same plant (Figure 1a). To investigate the impact of twig age on phytochemical composition, an untargeted metabolomic analysis was conducted, detecting 13 008 ion features in negative mode and 20 735 ion features in positive mode, respectively (Table S1). A total of 1662 annotated compounds were assigned to different metabolic pathways (Table S2). The metabolite profiling of different twig samples displayed dramatic variations in their chemical components (Figure 1b). PCA showed that PC1 and PC2 explained 40.17% and 10.73% of the variation, respectively (Figure 1c). The numbers of DAMs in different comparisons were shown in Figure 1d.

The top three largest KEGG terms were 'biosynthesis of phenylpropanoids' (38 metabolites), 'phenylalanine metabolism' (32 metabolites), and 'glycerophospholipid metabolism' (24 metabolites, Figure S1). According to the metabolite database, the largest number of identified metabolites were belonging to the 'lipids and lipid-like molecules', followed by 'benzenoids', 'organoheterocyclic compounds', and 'phenylpropanoids and polyketides' terms (Figure S2). Pearson's correlation coefficient analysis indicated well repeatability of the HPLC/MS data (Figure S3). Several quality control parameters, such as average *m/z*, retention time, and TIC, were analysed, indicating high-quality raw MS data (Figure S4a,b). To screen age-specifically accumulated metabolites, DAMs were grouped into 10 clusters, representing different accumulation patterns. Cluster I contained the metabolites that decreased with twig ages, while Cluster II contained the metabolites that increased with twig ages. Metabolites belonging to Cluster III–VII were specifically accumulated in Y1-5 samples, respectively (Figure S4c). Predominant metabolites in the Cluster I were oxidation–reduction-related compounds and predominant metabolites in the Cluster II were alkaloids. Interestingly, flavonoids were predominantly accumulated in the Y1 samples, terpenoids were predominantly accumulated in the Y3 and Y4 samples, and amino acids were highly accumulated in the Y5 samples (Figure S4d).

2.2 | Variations in Gene Expression Profiling Among Twigs of Different Ages

To reveal the variations in gene expression, transcriptomic analysis performed, yielding 88.34 Gb of raw data (Table S3). Pearson's correlation coefficient analysis indicated well repeatability of the RNA sequencing data (Figure S5). In total, 50 919 genes were detected, including 24 275 GO-annotated genes and 9400 KEGG

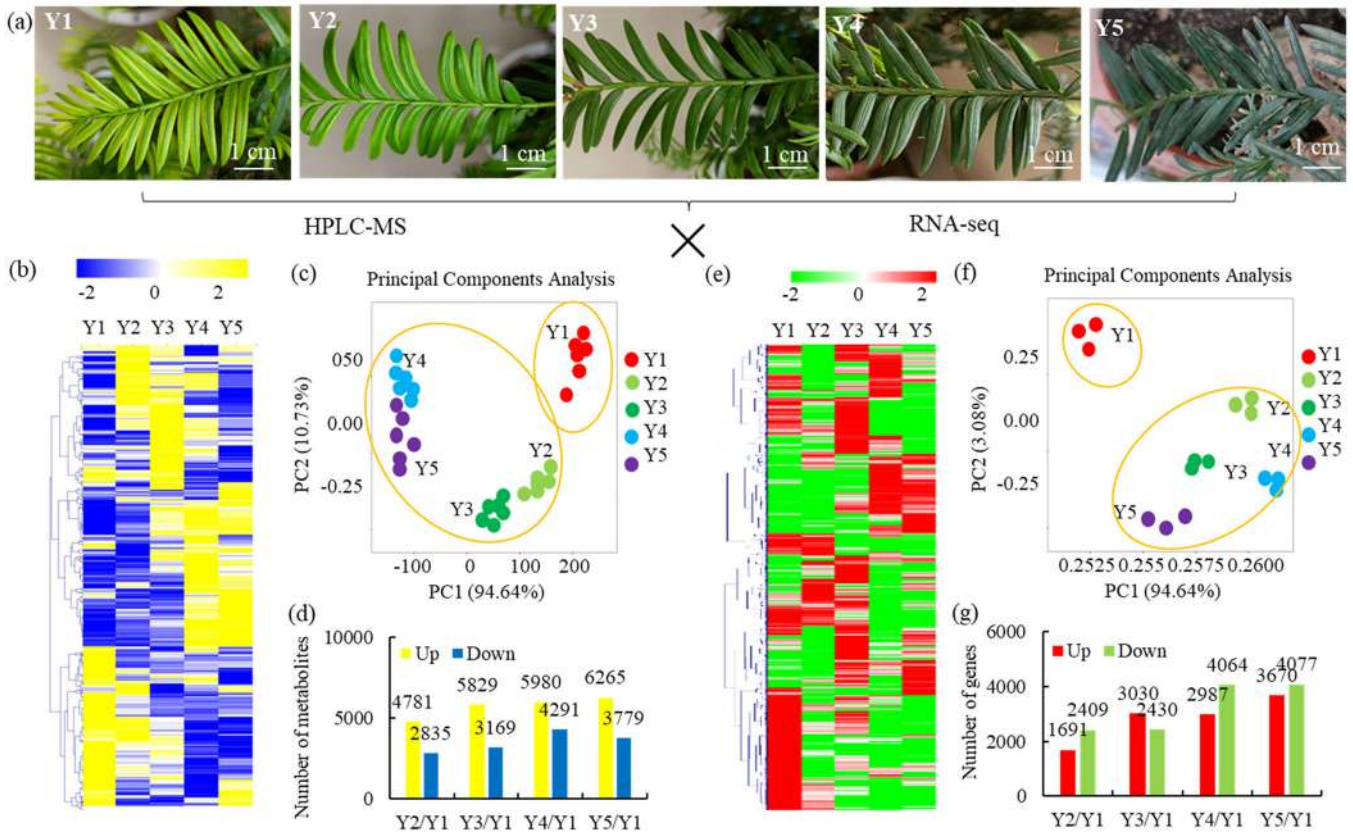

FIGURE 1 | Integrated untargeted metabolomic and transcriptomic analysis identified differences among twigs of different ages. (a) Five sample groups of twigs with different ages: 1-year-old (Y1), 2-year-old (Y2), 3-year-old (Y3), 4-year-old (Y4), and 5-year-old (Y5). Bars indicate 1 cm. (b) A heatmap of the abundance of metabolites in the five stem sections ($N = 6$). The heatmap scale ranges from −2 to +2 on a $\log_2$ scale. (c) PCA of the metabolomes from different sample groups. (d) Number of DAMs in various comparisons. (e) A heatmap of the gene expression in the four stem tissues ($N = 3$). The heatmap scale ranges from −2 to +2 on a $\log_2$ scale. (f) A PCA of the transcriptomes from five sample groups. (g) The number of the DEGs in different comparisons. [Color figure can be viewed at wileyonlinelibrary.com]

annotated genes (Table S4). A heatmap showed the gene expression profiles of twigs with different ages (Figure 1f). PCA showed that PC1 and PC2 explained 94.64% and 3.08% of the variation, respectively (Figure 1g).

The numbers of DEGs in different comparisons are presented in Figure 1h. GO enrichment analysis was performed to predict the biological functions that the DEGs were involved in (Figure S6a). Most of the DEGs enriched in several Taxol biosynthesis-related GOs (GO:0042616 and GO:0036203), hormone response-related GOs (GO:0009938, GO:0009723, GO:0009867, and GO:0080151), and shoot development-related GOs (GO:0032502, GO:0080186, GO:0090351, and GO:0048367). Our data suggest great changes in Taxol biosynthesis and hormone signalling occur during the twig development process (Figure S6b). KEGG enrichment analysis suggested that the DEGs were enriched in lipid metabolism, terpenoid metabolism, and flavonoid metabolism pathways (Figure S6c).

2.3 | Integrated Metabolomic and Transcriptomic Analysis of Taxol Biosynthesis in *T. mairei*

Taxol biosynthesis pathway involves several intermediate metabolites and enzymes (Figure 2a). In our study, Taxol and 13 intermediate metabolites were detected through untargeted metabolomic analysis. GGPP, an important precursor for Taxol biosynthesis, was highly accumulated in the Y3-5 samples. Taxol and most of its intermediate metabolites, such as 10-deacetyl-2-debenzoylbaccatin III, 10-deacetylbaccatin III, and baccatin III, were predominantly accumulated in the Y1 samples (Figure 2b). Additionally, a number of Taxol biosynthesis-related genes were identified, including three *TS* genes, five *T5OH* genes, five *T13OH* genes, six *TAT* genes, five *T10OH* genes, two *TBT* genes, one *DBAT* gene, one *DBTNBT* gene, two *T7OH* genes, and one *T2OH* gene. Most of the Taxol biosynthesis-related genes were significantly decreased with twig ages, suggesting that Taxol biosynthesis is more active in young twigs than in old twigs (Figure 2c).

2.4 | Differences in the Community Structure of Endophytic Microorganisms

ITS sequencing obtained 2 404 688 raw tags, yielding 3,129 ASVs (Table S5). Sequence length ranged from 200 to 400 bp (Figure S7a). Venn diagram showed that only 29 common ASVs were detected in all the sample groups (Figure S7b). Alpha and beta diversity analysis confirmed that the communities of endophytic fungi were significantly affected by twig age (Figure 3a,b). Furthermore, the hierarchical clustering analysis indicated that twig samples with different

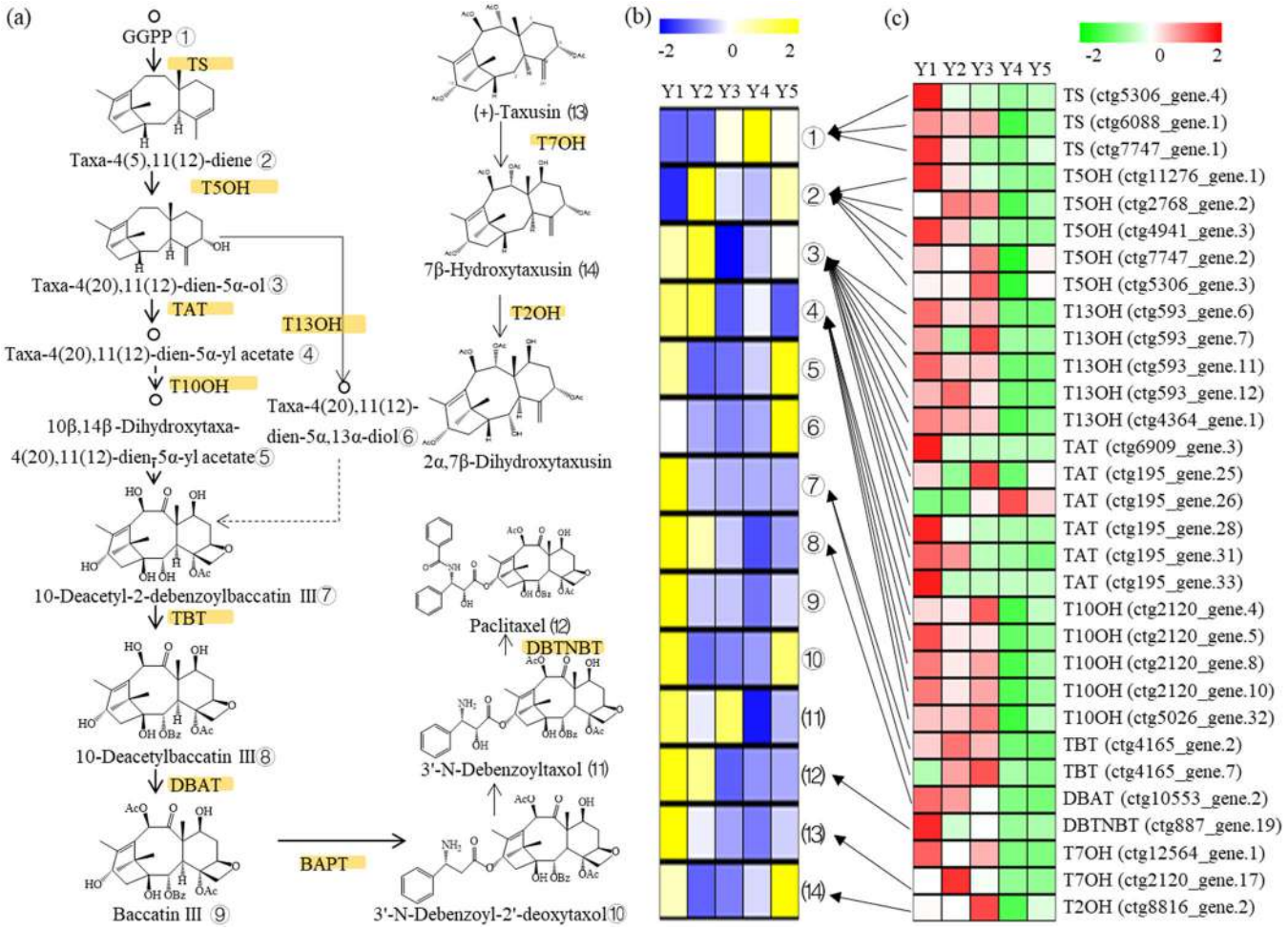

FIGURE 2 | Integrated metabolomic and transcriptomic analyses for Taxol biosynthesis. (a) Diagram of the classic Taxol biosynthesis pathway. The numbers in parentheses represented the number of coding genes for each enzyme. (b) Differential accumulation of several metabolites related to the taxol pathway among the five sample groups. The numbers in the circle represent different metabolites, consistent with that in part a. The colour scale ranges from −2 to +2 on a $\log_2$ scale. (c) Expression analysis of genes encoding enzymes related to the paclitaxel biosynthesis pathway among the five sample groups. The colour scale ranges from −2 to +2 on a $\log_2$ scale. [Color figure can be viewed at wileyonlinelibrary.com]

ages were well separated, and the Y1 group has greater differences compared to the other four twig groups (Figure 3c).

According to the ASV sequences, all endophytic fungi were predicted and grouped into 433 genera. Only 65 fungal genus were detected in the Y1 group, and more than 200 fungal genera were detected in the Y3–Y5 groups (Figure 3d), suggesting that the old twigs contained more endophytic fungi than the young twigs. To determine the effects of age on fungal communities, linear discriminant analysis coupled with the effect size analysis (LEfSe) analysis was performed to identify biomarker taxa in different twig groups (Figure 3e). The relative abundance of all fungal genera is shown in Figure 3f. In the Y1 group, *Davidiella*, *Pleosporales*, and *Malassezia* were the dominant fungal genera; in the Y2 and Y3 groups, *Cladosporium*, *Davidiella*, and *Alternaria* were the dominant fungal genera; and in the Y4 and Y5 groups, *Didymellaceae*, *Cladosporium*, and *Davidiella* were the dominant fungal genera.

The relation between the differential fungal genus and the differentially accumulated taxoids in the host plant was analysed. Pearson correlation analysis screened a series of taxoid biosynthesis-related fungal genus, such as *Guignardia*, *Cladosporium*, *Nigrospora*, *Didymella*, *Phomopsis*, *Botryosphaeria*, *Chaetomium*, *Phanerochaete*, *Aspergillus*, *Alternaria*, *Paraconiothyrium*, and *Phyllosticta* (Figure 3g).

2.5 | Influence of Taxoids on the Growth of Endophytic Fungi Isolated From *T. mairei* Twigs

We have previously screened and obtained a large number of endophytic fungal isolates from the twig of *T. mairei* (Table S6). The above correlation analysis provided us with cues for screening Taxol biosynthesis-related endophytic fungi. To analyse the role of endophytic fungi in age-associated Taxol biosynthesis, 11 typical fungi, including M5 (*Alternaria*), N16 (*Cladosporium*), J02 (*Diaporthe*), M11 (*Didymella*), L01 (*Guignardia*), N13 (*Nigrospora*), N42 (*Paraconiothyrium*), M8 (*Perenniporia*), R01 (*Phanerochaete*), J10 (*Phomopsis*), and L13 (*Phyllosticta*), were selected (Figure 4a). The relative abundance of the selected endophytic fungi from different twig groups was analysed according to the ITS sequencing data (Figure S8).

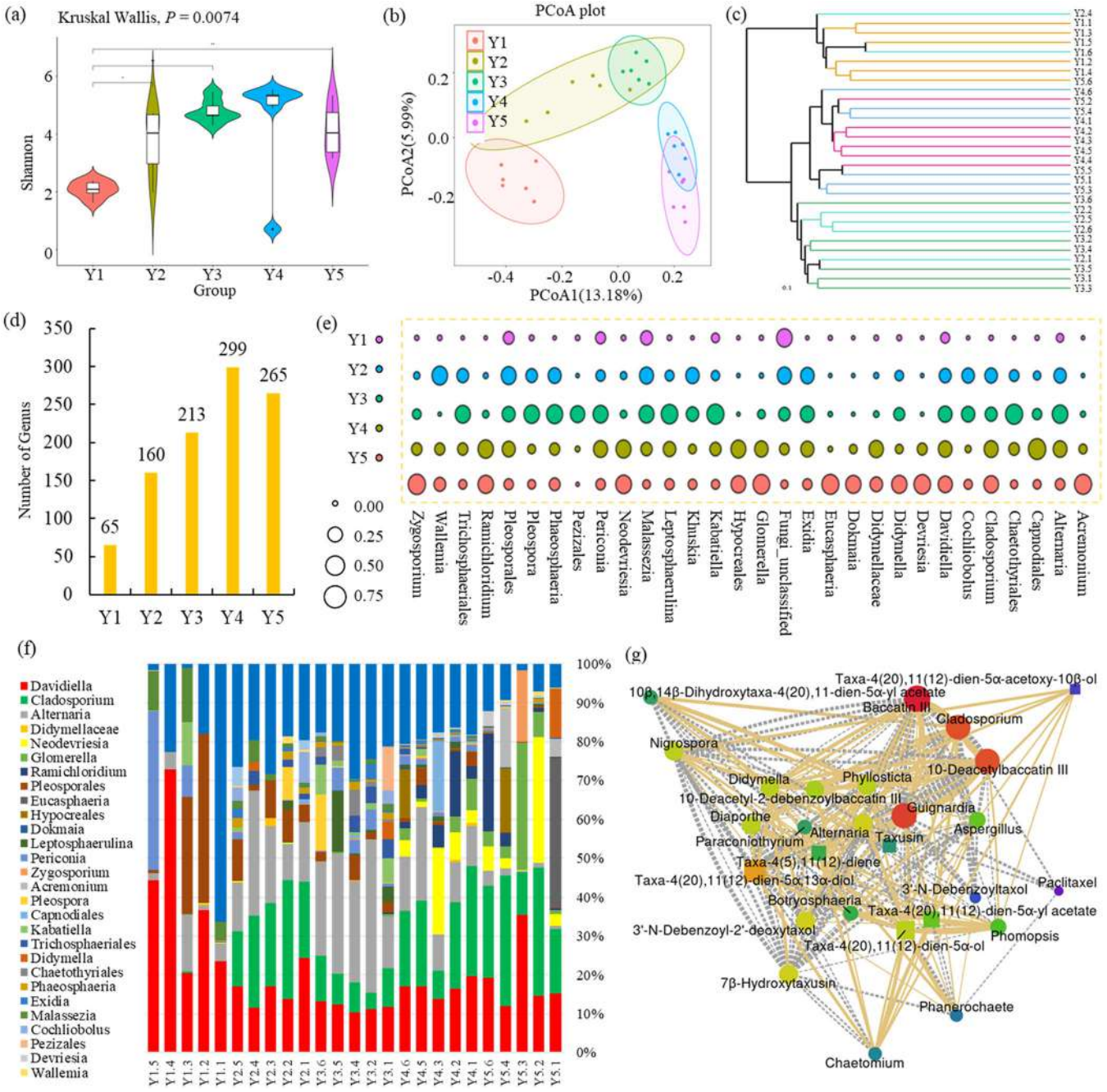

FIGURE 3 | Differences in community structure of endophytic fungi among different sample groups. (a) Analysis of alpha diversity by Shannon index. (b) Analysis of beta diversity by PCoA clustering. (c) UPGMA clustering analysis of the endophytic communities. (d) Number of fungal genus detected in different sample groups. (e) The relative abundance of endophytic fungi in different sample groups. (f) Analysis of the differential fugal genus in different sample groups. (g) Pearson correlation analysis of differential fungal genus and host's Taxol levels. [Color figure can be viewed at wileyonlinelibrary.com]

To analyse/detect the inhibitory effect of taxoids on the endophytic fungal growth, dilution agar assays were performed. Taxol significantly inhibited the growth of L01, R01, N16, M8, and M11 compared to DMSO used control group ($p < 0.05$); BAC significantly inhibited the growth of L01, J02, R01, N16, M8, N13, and M5 compared to DMSA used control group ($p < 0.05$); and 10-Deacetylbaccatin III (DAB) significantly inhibited the growth of J10, R01, N16, M8, M11, and L13 compared to DMSA used control group ($p < 0.05$). Our data showed that three taxoids (Taxol, Baccatin III (BAC), and DAB) greatly influence the growth of most of the selected typical endophytic fungi (Figure 4b).

2.6 | Effect of Inoculation With Different Endophytic Fungi on the Host's Metabolite Accumulation

Based on the correlation between endophytic fungi and Taxol biosynthesis, we are striving to develop new fungal elicitors (Figure 5a). In total, 7029 ion features with annotation were identified (Table S7). Quality control of the ion feature data was analysed by various methods. Boxplot analysis showed that the median values of different sample groups are relatively consistent (Figure S9a). PCA results showed that endophytic fungi-treated groups displayed great

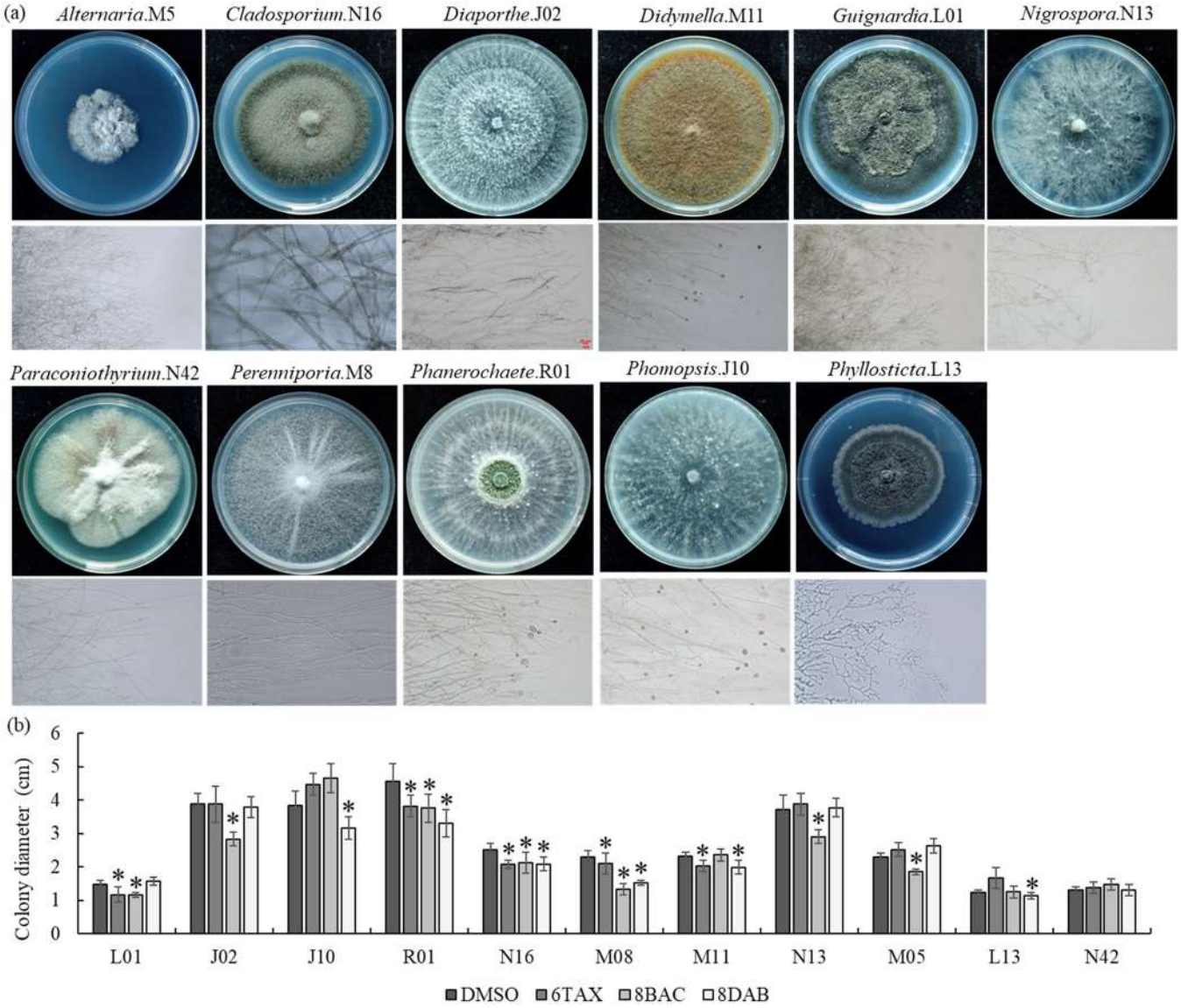

FIGURE 4 | Screening and isolation of Taxol metabolism-associated endophytic fungi. (a) The isolated endophytic fungal isolates were observed in plates. (b) The effect of taxoids on the growth of endophytic fungi isolated from *T. mairei*. A positive percentage represents the inhibition rate, while a negative percentage represents the promotion rate. "*" indicated the significant differences between the taxoid and DMSO treatments. [Color figure can be viewed at wileyonlinelibrary.com]

differences to the control group (Figure S9b). Treeplot analysis indicated good data repeatability in one group (Figure S9c). A heatmap showed the metabolite accumulation profiles of twigs with different fungi incubations (Figure 5b). Most of the identified metabolites were grouped into different subclasses, including 8.51% of amino acids, 7.88% of carbohydrates, 2.05% of diterpenoids, 3.82% of fatty acids, 1.93% of fatty acyl glycosides, 4.02% of flavonoids, 1.95% of steroidal glycosides, 2.94% of terpene glycosides, and 1.87% of triterpenoids (Figure 5c). Compared to the control group (CK), a number of DAMs were detected, ranging from 578 DAMs (L13/CK) to 735 DAMs (R01/CK), suggesting that R01 causes the greatest changes in the metabolic profile of *T. mairei* (Figure 5d). KEGG classification analysis identified 112 diterpenoids, only 16 ~ 21 of these were significantly changed by endophytic fungi incubations ($p < 0.05$) (Figure 5e). Twelve taxoids, belonging to the subclass of diterpenoids, were identified, 7 ~ 8 of which were significantly ($p < 0.05$) altered by endophytic fungi incubations (Figure 5f). Our data suggest that taxoids are a class of diterpenoid compounds that specifically respond to fungal inoculations compared to the control group. More than half of the 12 detected taxoids, such as 10-deacetylbaccatin III, taxol, taxine B, baccatin III, and taxusin, were significantly ($p < 0.05$) upregulated by various fungi inoculations. No significant changes were observed in the levels of cephalomannine, cabazitaxel, docetaxel, and taxol C (Figure 5g).

2.7 | Effect of Endophytic Fungi Inoculation on the Host's Gene Expression and Hormone Accumulation

The effect of endophytic fungi inoculation on Taxol accumulation was evaluated, gaining two efficient fungal elicitors (Figure 6a). To reveal the regulation mechanism of Taxol biosynthesis, two efficient fungal elicitors, *Guignardia* L01 and

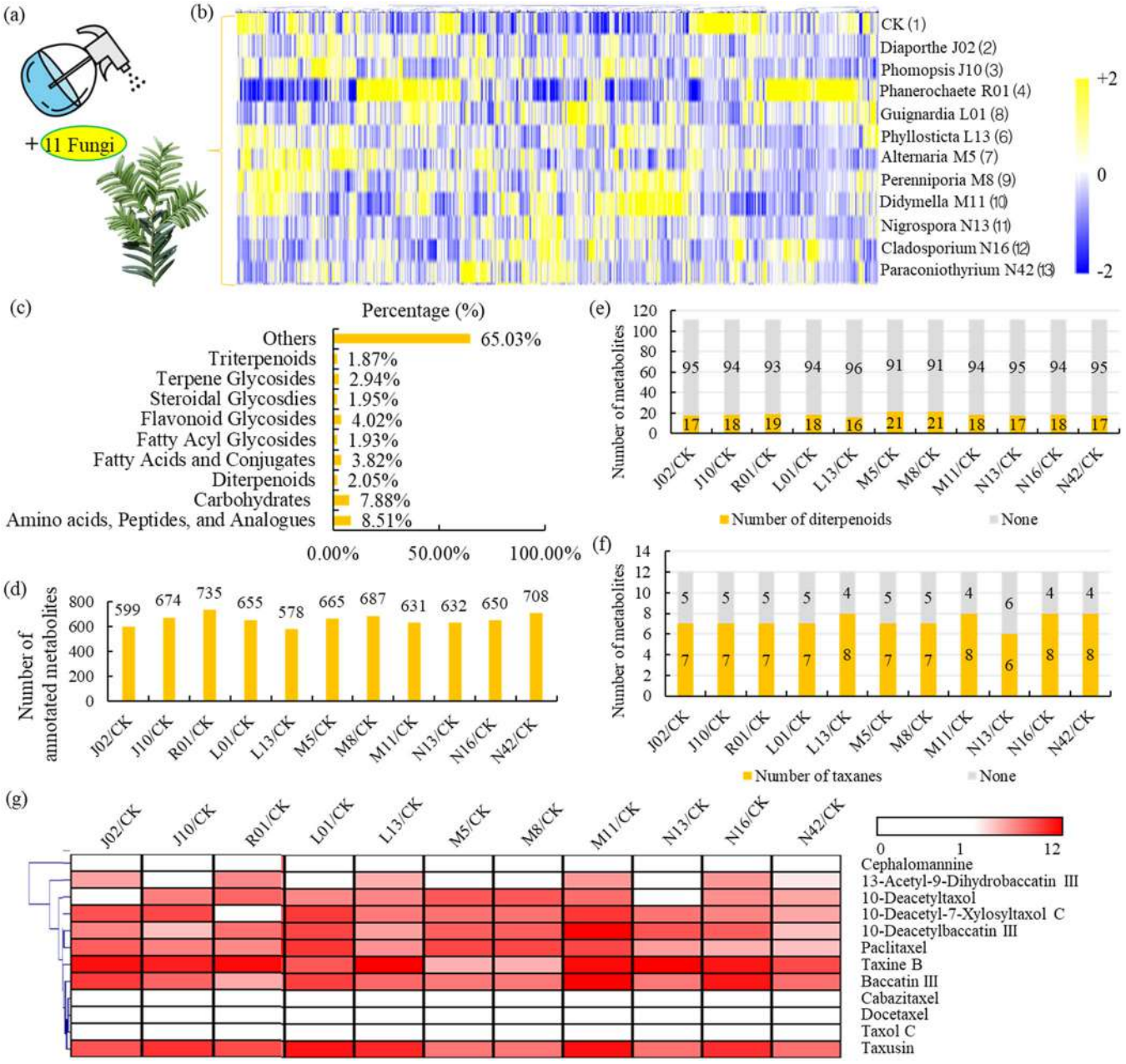

FIGURE 5 | Effect of inoculation with different endophytic fungi on the host's metabolism. (a) Co-inoculation of *Taxus* twigs with different endophytic fungi. (b) Heatmap showing the relative accumulation levels of each detected metabolite under different endophytic fungi inoculations. The heatmap scale ranges from −2 to +2 on a $\log_2$ scale. (c) The number of differentially accumulated metabolites under different endophytic fungi inoculations. (d) Enrichment analysis of several secondary metabolism-related GO terms. (e) The number of differentially accumulated diterpenoids under different endophytic fungi inoculations. (f) The number of differentially accumulated taxanes under different endophytic fungi inoculations. (g) The contents of taxoids under different endophytic fungi inoculations. [Color figure can be viewed at wileyonlinelibrary.com]

Diaporthe J02, were selected for inoculation assays (Figure 6b). HPLC data indicated that the two fungi (L01 and J02) cannot synthesise Taxol (Figure S10). After 48 h incubation, the twigs of *T. mairei* were harvested and washed with ddH_2O for untargeted transcriptomic analysis. In total, 1856 DEGs, including 1103 up- and 753 downregulated genes, after L01 incubation, and 1757 DEGs, including 1142 up- and 615 downregulated genes (Figure 6b). Interestingly, most of the DEGs were commonly identified in both of the L01/CK and J02/CK comparisons, suggesting that the two fungal elicitors have similar effects on the host's gene expression (Figure S11).

GO enrichment analysis showed that a number of DEGs were enriched in various Taxol biosynthesis-related GO terms (Figure 6c). Fungal elicitors enhanced the Taxol accumulation by activating the Taxol biosynthesis pathway. Interestingly, several hormone signalling pathways were also greatly activated by fungal elicitors. For example, four ABA signalling-related GO terms, including '(+)-abscisic acid 8′-hydroxylase activity', 'abscisic acid binding', 'abscisic acid-activated signalling pathway', and 'abscisic acid catabolic process', were significantly enriched under fungal elicitor treatments (Figure 6c). Additionally, four

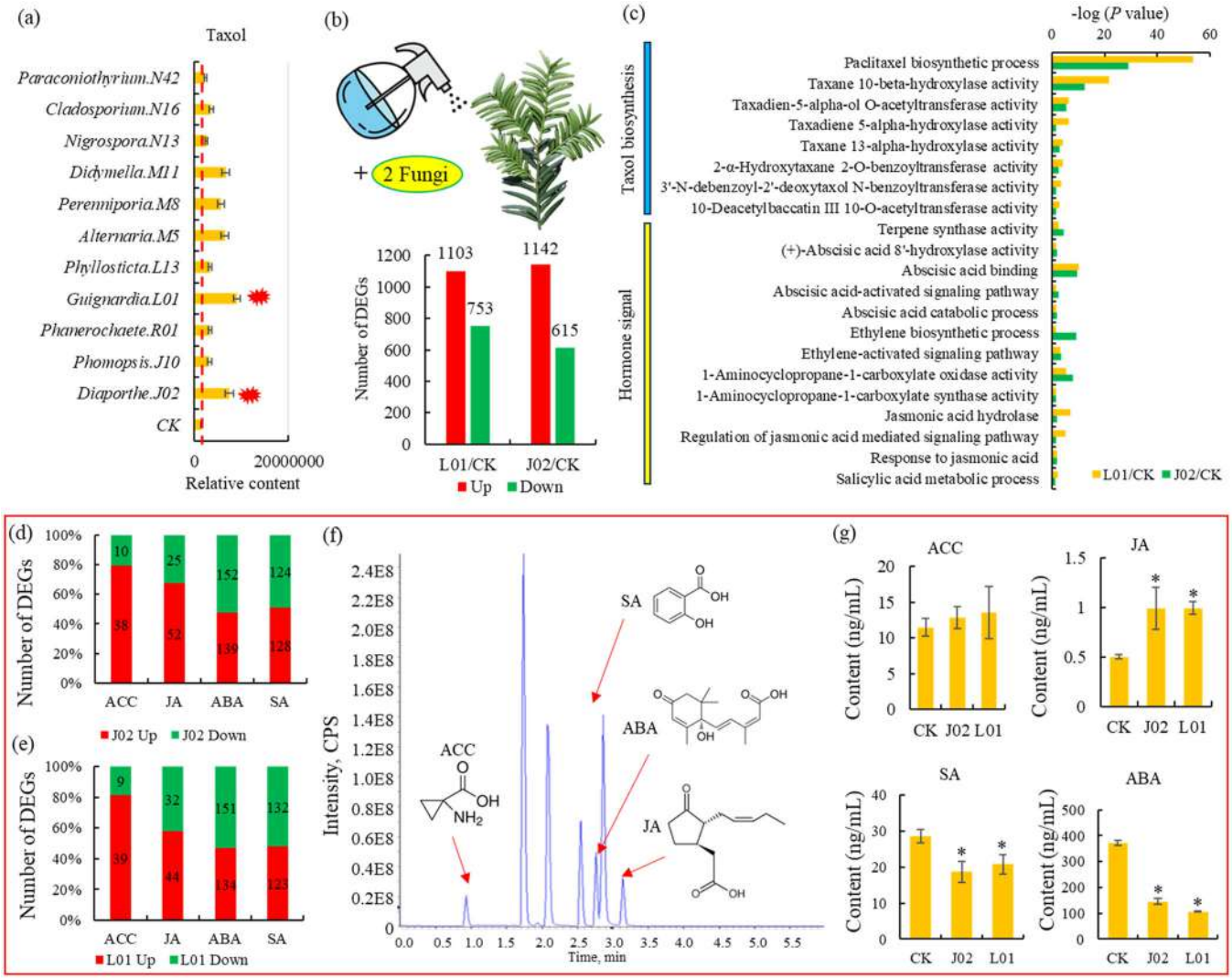

FIGURE 6 | Effect of inoculation with two selected endophytic fungi on the host's gene expression. (a) The taxol content in *Taxus* twigs under different endophytic fungi inoculations. Red stars indicated two efficient fungal elicitors. (b) The number of DEGs under two different endophytic fungi inoculations. (c) Enrichment analysis of taxol biosynthesis- and hormone signal-related GO terms. (d, e) The number of hormone-related DEGs under the J02 and L01 inoculations. (f) The HPLC chromatogram of four selected phytohormones, including ACC, SA, ABA, and JA. (g) Contents of four important phytohormones in *Taxus* twigs under the two endophytic fungi inoculations. "*" indicates significant differences between control and treatment groups at $p < 0.05$. [Color figure can be viewed at wileyonlinelibrary.com]

ethylene signalling-related GO terms, three JA signalling-related GO terms, one BR-related GO, one GA-related GO, and one SA-related GO, were significantly altered under fungal elicitor treatments. Expression analysis showed that most of the ethylene and JA signalling pathway-related genes were upregulated by the J02 and L01 incubations (Figure 6d–f).

The contents of four important phytohormones, including ACC, JA, SA, and ABA, were determined through target metabolomic analysis (Figure 6f). No significant changes were observed in the ACC contents between the CK and J02/L01-treated groups. Interestingly, the levels of endogenous JA were significantly upregulated and the levels of endogenous SA and ABA were significantly downregulated under the J02/L01 incubations (Figure 6g). Our data suggest that endogenous JA might play a significant role in fungi elicitor-mediated regulation of Taxol biosynthesis.

2.8 | Identification of a JA Signal-Related MYC2a

According to the *T. mairei* genome, four MYC2 subfamily members were identified. Expression analysis revealed that *MYC2a* was significantly upregulated under the J02/L01 inoculations (Figure 7a). The full-length encoding sequence of MYC2a was cloned through PCR amplification. A phylogenetic tree was constructed to analyse the relationship of MYC2 proteins between *T. mairei* and other plants (Figure 7b). Multiple sequence alignment indicated that *T. mairei* MYC2a is conserved in the HLH domain in comparison with other MYC family members (Figure 7c).

2.9 | MYC2a Plays a Potential Regulatory Role in Taxol Biosynthesis

A series of Taxol biosynthesis-related genes were significantly induced by two selected fungal elicitors. Expression analysis showed

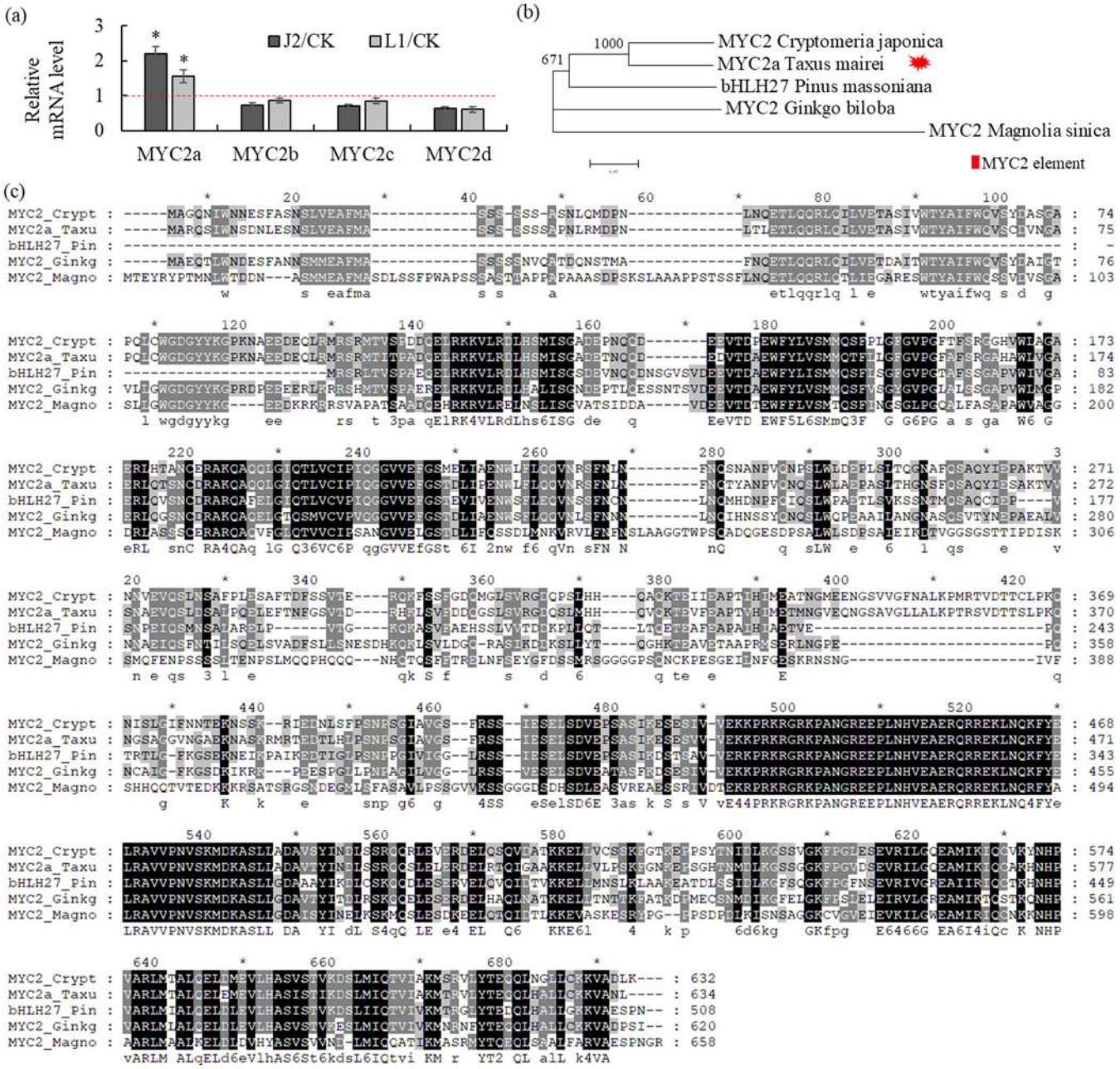

FIGURE 7 | Identification of JA signal pathway-related TF, MYC2a. (a) Relative expression level of MYC2 subfamily TF genes under J02 and L01 inoculations. '*' indicated significantly changed *MYC2* subfamily gene under the J02 and L01 inoculations ($p < 0.05$). (b) Evolutionary analysis of *T. mairei* MYC2a and other known MYC2 proteins in plants. (c) Multiple sequence alignment analysis of MYC2 family members. [Color figure can be viewed at wileyonlinelibrary.com]

that two *TS* genes (ctg5306_gene.4 and ctg7747_gene.1), two *T5OH* genes (ctg11276_gene.2 and ctg4941_gene.1), one *T13OH* gene (ctg593_gene.12), one *TAT* gene (ctg6909_gene.2), one *TBT* gene (ctg5026_gene.7), one *DBAT* gene (ctg887_gene.19), one *DBTNBT* gene (ctg195_gene.25), two *T7OH* genes (ctg12564_gene.1 and ctg2120_gene.17) were upregulated by fungal elicitors by more than fivefolds (Figure 8a).

To predict potential targets of MYC2a, the promoter sequences of 11 fungal elicitor responsive Taxol biosynthesis-related genes were scanned for the MYC2 binding elements. Interestingly, the promoters of *T5OH* (ctg11276_gene.1), *DBTNBT* (ctg195_gene.25), *T7OH* (ctg2120_gene.17), *TS* (ctg5306_gene.4), *T13OH* (ctg593_gene.12), *TS* (ctg7747_gene.1), and *DBAT* (ctg887_gene.19) contained at least one tandem MYC binding element, and were predicted as potential targets of MYC2a (Figure S12). Electrophoretic mobility shift assay (EMSA) results showed that MYC2a bound directly to the target element in the promoters of *DBTNBT* (ctg195_gene.25), *T7OH* (ctg2120_gene.17), *TS* (ctg5306_gene.4), *T13OH* (ctg593_gene.12), and *TS* (ctg7747_gene.1), suggesting they were potential target genes of MYC2a (Figure 8b–e). No significant binding activities were observed in the MYC2a-*T5OH* and MYC2a-*DBAT* pairs. To determine the transcriptional activity of MYC2a, a dual-luciferase (LUC) reporter assay was carried out using a transient expression. The dual-LUC data confirmed the transcriptional activation effect of MYC2a on *DBTNBT*, *T7OH*, *TS*, *T13OH* genes

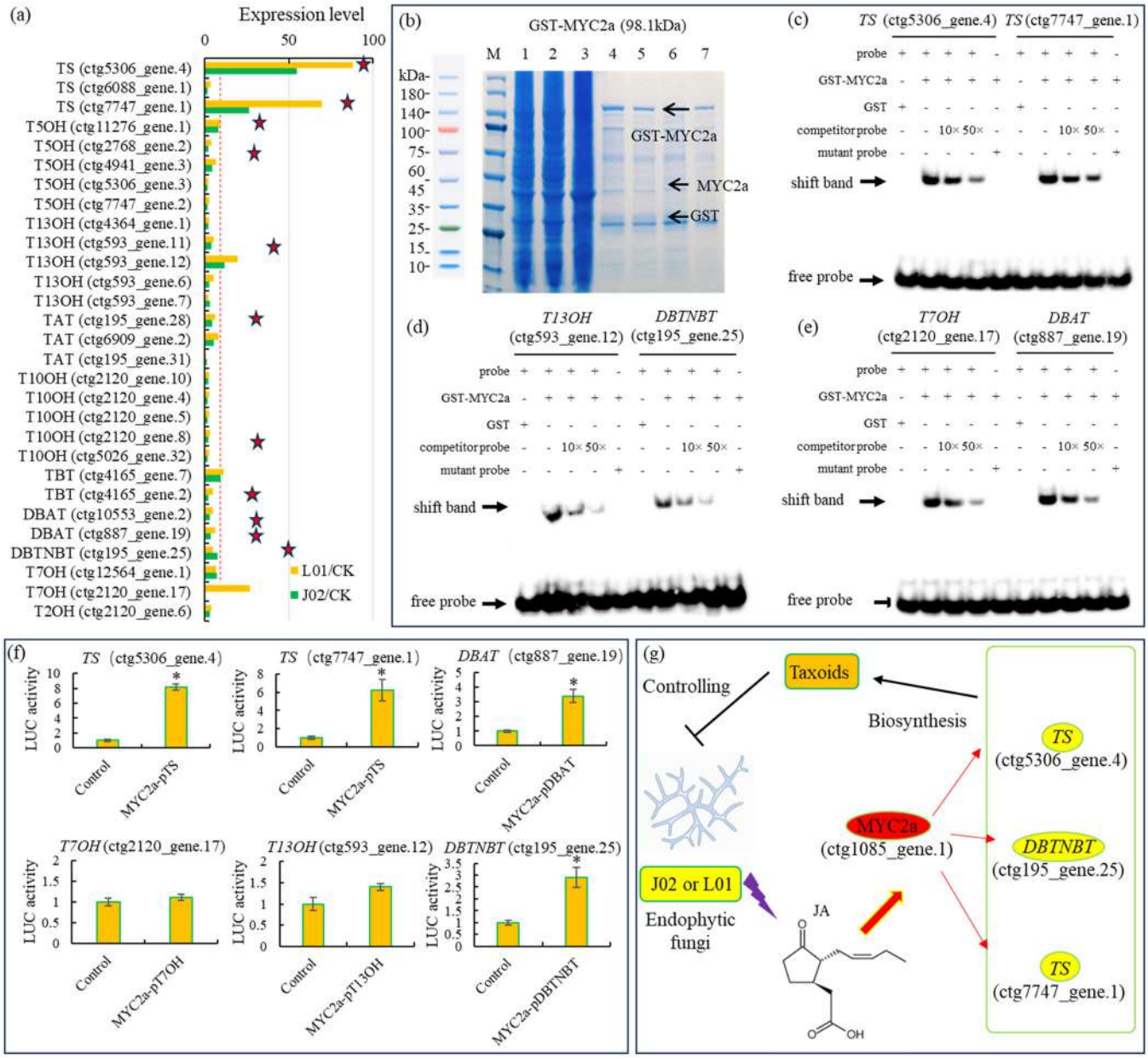

FIGURE 8 | A potential regulatory network involved in the fungal elicitor-activated Taxol biosynthesis pathway. (a) Expression analysis of the Taxol biosynthesis pathway genes under L01 and J02 inoculations. (b–e) EMSA analysis of the binding sites of MYC2a to its potential targets. GST only or the TF-GST fusion protein was incubated with the probes containing the binding elements derived from the promoters. '−' and '+' represent absence and presence, respectively, and 20◊ and 200◊ show increasing amounts of probes for competition. (f) The dual-luciferase assays in tobacco leaves showed that co-transformation of TFs activates the promoters of taxol biosynthesis-related genes. '*' indicates significant differences between control and treatment groups at $p < 0.05$. (g) A model for the role of MYC2a in controlling the structure of endophytic fungi. [Color figure can be viewed at wileyonlinelibrary.com]

(Figure 8f). Our data provided a potential regulatory network involved in the fungal elicitor-activated Taxol biosynthesis pathway (Figure 8g).

3 | Discussion

3.1 | Twig Age Affected the Secondary Metabolism and Endophytic Fungi Assemble of the Host *Taxus* Tree

There is convincing evidence of a link between tissue age and secondary metabolism in perennial plants. Plant age affected the accumulation of various types of secondary metabolites, including flavonoids and anthocyanins in *Batavia lettuce*, annatto pigments in *Bixa orellana*, and ABA and anthocyanins in *Aristotelia chilensis* (Machado et al. 2023; Escrich et al. 2021; Sng et al. 2021). However, there are no reports on the correlation between tissue age and the accumulation of Taxol. In the present study, an integrated metabolomic and transcriptomic analysis revealed the predominant accumulation of Taxol in young twigs of *Taxus* trees, indicated that young twigs are more suitable for the industrial extraction of Taxol.

The plant's endophytic fungi play an essential role in enhancing host development and secondary metabolism (Yan et al. 2019). The colonisation and assembly of endophytes

are significantly affected by the host's genotypes and environmental stresses (Latz et al. 2021). Interestingly, the impacts of tissue age on the host's microbial assembles were reported in various plants. Seasonal and leaf age-dependent variations in the endophytic fungal assemblages were observed in *Camellia japonica* (Osono 2008). In *Swietenia macrophylla*, the percentage of antimicrobial activity-associated isolates increased with leaf age (Ibrahim, Lee, and Sheh-Hong 2014). Recently, the spatial and temporal dynamics of bacterial community assembly were surveyed during the *Arabidopsis* development process (Beilsmith, Perisin, and Bergelson 2021). In *T. mairei*, only 65 genera were observed in the youngest twig sample and more than 200 genera were observed in old twigs, confirming the effect of twig age on endophytic fungal assemblies.

3.2 | The Biological Function of Taxoids in *Taxus* Trees

Taxol is a significantly effective anticancer drug used for the treatment of various cancers (Yu et al. 2023). However, the biological function of taxoids for *Taxus* trees themselves is rarely explored. The synthesis of Taxol is an extremely complex and energy-consuming biosynthesis process, involving over 30 steps (Kaspera and Croteau 2006; Zhan et al. 2023). *Taxus* trees cannot effortlessly synthesise taxoids solely for the sake of human health. We hypothesised that endogenous taxoids, just like balance valves, may have a specific effect on controlling the microbiota assembly in *Taxus* trees. Plant-derived diterpenoids are often considered fungicides with significant antifungal activity (Adamczyk et al. 2023). The reproduction of many endophytic fungi is inhibited by taxoids, confirming the antifungal activity of taxoids. Our data explained the negative correlation between taxoid content and the complexity of the endophytic fungal community in twigs of varying ages. It is interesting that M8 is strongly inhibiting by all tested taxoids, but its level is very low in old twigs. Conversely, L13, less sensitive to taxoids, was found predominantly in Y5-stage twigs. It indicated that there is another mechanism involved in the interaction between fungi and plant secondary metabolism. *Taxus* tree synthesises taxoids to control the population of specific genera of endophytic fungi in the young twigs, indicating that these specific genera can be utilised as fungal elicitors to activate the biosynthesis pathway of taxoids.

3.3 | Discovery of Two New Efficient Fungal Elicitors Involved in Taxol Biosynthesis

Using omic correlation analysis, we predicted several potential fungal elicitors related to Taxol biosynthesis. To date, many studies have focused on screening and studying Taxol-producing fungi (Cheng et al. 2022). For example, *Aspergillus aculeatinus*, *Alternaria alternata*, and *Cladosporium cladosporioides* were reported to be Taxol-producing fungi (Fu et al. 2023; Miao et al. 2018; Qiao, Tang, and Ling 2020). Although the fungi selected in our study do not produce Taxol, they are potential fungal elicitors of Taxol biosynthesis. Fortunately, two efficient fungal elicitors, L01 (*Guignardia*) and J02 (*Diaporthe*), were identified, increasing the Taxol contents by 5.91- and 4.83-folds, respectively. The strains from the *Guignardia* genus are the dominant endophytes in the leaves of various woody plants (Fan et al. 2020; Xiong et al. 2013). The *Guignardia* and *Diaporthe* genera contain many beneficial endophytic fungi with various functions. Cocultivation with a *Guignardia* genus endophyte specifically affected the growth and chemical composition of *Dendrobium catenatum* (Wu et al. 2020). Inoculation with a *Diaporthe* fungal endophyte from a perennial grass adapted to rocky sea cliffs improved the growth and salinity tolerance of gramineous crops (Toghueo et al. 2022). Our data revealed novel functions for the two endophytic fungi mentioned above, which can serve as fungal elicitors to induce the biosynthesis of Taxol in *Taxus* twigs.

3.4 | Endogenous Hormones Play an Essential Role in Fungal Elicitor-Mediated Taxol Biosynthesis in the Host *Taxus* Trees

In our study, the J02 and L01 fungal elicitors significantly activated various Taxol biosynthesis-related GO terms, leading to an increase in the content of Taxol. Interestingly, various hormone-related GO terms were also changed under the J02 and L01 inoculations, indicating an essential role of hormone signalling pathways in fungal elicitor-mediated Taxol biosynthesis. Several hormones, such as JA, ABA, GA, and ET, were reported to be involved in Taxol biosynthesis (Cao et al. 2022; Demidova et al. 2023). Jiang's study showed that the endophytic fungus *Pseudodidymocyrtis lobariellae* KL27 promotes Taxol biosynthesis and accumulation by activating the JA biosynthesis and JA signal transduction pathways (Cao et al. 2022). Despite significant changes in the expression of ethylene signalling-related genes, the content of ACC was not affected by the J02 and L01 inoculations. JA contents were significantly upregulated by both of the J02 and L01 inoculations, confirming the role of JA in fungal elicitor-activated Taxol biosynthesis. JA is essential for diverse plant defence responses against biotic and abiotic stresses (Li et al. 2021). Plants perceive the treatment of fungal elicitor as a potential threat, prompting the activation of the JA signalling pathway to boost their resistance to environmental stresses. In the future, the induction or inhibition of JA signalling pathways will be a key concern for screening new effective fungal elicitors.

3.5 | The Regulatory Network of Fungi Elicitor-Activated Taxol Biosynthesis

MYC2, a key transcriptional regulator in the JA signalling significantly contributes to in enhanced improved biosynthesis of plant secondary metabolites (Liu et al. 2022). Previous studies have investigated the function of MYC2 in Taxol biosynthesis in various *Taxus* species (Cui et al. 2019). In *T. mairei*, four MYC2-like genes were identified, one of which was significantly upregulated by the J02 and L01 inoculations. We speculated that MYC2a might be a key transcription regulator of fungal elicitor-activated Taxol biosynthesis.

In *T. chinensis*, overexpression of MYC2a significantly increased the expression of *TS*, *TAT*, *DBTNBT*, *T13OH*, and *T5OH* genes (Zhang et al. 2018). In *T. media*, MYC2 showed transcriptional activation activity on the promoters of *DBTNBT*, *T2OH*, *T7OH*, *T5OH*, *T13OH*, *DBAT*, *T10OH*, *PAM*, *GGPPS*, and *TS* (Cui et al. 2019).

Considering the expression levels and promoter regulatory elements, a series of Taxol biosynthesis pathway genes, such as *T13OH*, *TS*, *DBTNBT*, and *T7OH*, were predicted to be the downstream targets of MYC2a. Regardless of the *Taxus* species, MYC2 is a key factor in regulating the biosynthesis of paclitaxel.

3.6 | New Ideas for Screening Fungal Elicitors of Taxol Biosynthesis

Fungal elicitors have been reported as an impressive strategy for enhancing Taxol biosynthesis in various cell suspension systems (Salehi et al. 2021). Our data confirmed the inhibitory effect of taxoids on the growth of endophytic fungi, suggesting that taxoids are important regulators of the community structure of endophytic microorganisms. In young leaves, the concentration of Taxol is relatively high, which results in the growth inhibition of certain specific endophytic fungi. Taking advantage of the above phenomenon, we have screened several endophytic fungi. Fortunately, two fungal elicitors were obtained, which can be used in the research of the artificial induction of Taxol in a suspended cell system. It is worth mentioning that the endophytic fungi used have a low abundance level in young leaves, where the content of Taxol is high. It is suggested that effective fungal elicitors may be negatively correlated with Taxol content in *Taxus* trees.

4 | Conclusion

Using omic correlation analysis, a negative correlation between Taxol content and the complexity of the endophytic fungal community in twigs was predicted. We identified two effective fungal elicitors, L01 (*Guignardia*) and J02 (*Diaporthe*), which activate Taxol biosynthesis by regulating the MYC2a-controlled JA signalling pathway. Our data revealed the effect of twig age on the secondary metabolism of Taxus and provided a novel approach to screen effective fungal elicitors involved in Taxol biosynthesis. In future research, we will optimise the preparation of fungal elicitors, such as fungal cell walls, extracts, etc., hoping to obtain more efficient elicitors.

5 | Materials and Methods

5.1 | *Taxus* materials and treatments

T. mairei trees were planted in the growth chamber at Hangzhou Normal University, Hangzhou, China, at day/night temperature 23 ~ 26°C/16 ~ 18°C and photoperiod of 12 h. The twigs of different ages (Y1 for 1-year-old, Y2 for 2-year-old, Y3 for 3-year-old, Y4 for 4-year-old, and Y5 for 5-year-old) were harvested and stored for further analysis.

5.2 | Untargeted Metabolomic Profiling

About 60 mg of twigs from each sample group ($N = 6$) were treated with 600 μL of methanol-H_2O (V:V = 7:3, with a mixed internal standard) in a 1.5 mL centrifuge tube. The mixed samples were ground at 4°C for 2 min at a rate of 1500 strokes/min using the 2010 Geno/Grinder. The samples were homogenised and extracted with a 250 μL chloroform/methanol/water (1:3:1) working solution. After being vacuum-dried, the samples were resuspended in a methanol solution. The extract samples were uploaded and separated by Waters ACQUITY UPLC I-Class Plus/Thermo QE with an ACQUITY UPLC HSS T3 column. Then, the resulting samples were analysed using a high-resolution MS/MS TripleTOF 5600 Plus System according to a previously published work (Yu et al. 2018).

The ion features of MS/MS data were generated by SCMS software. The relative standard deviations of each ion feature were calculated according to the quality control samples. The ion features with deviations more than 30% were removed. The annotation information for each ion feature was generated by searching the online KEGG (https://www.kegg.jp/) and PLANTCYC (https://www.plantcyc.org/) metabolic databases.

5.3 | Standard Solutions and Calibration Curves for Targeted Hormones

All chemicals and solutions, such as methanol, acetonitrile, 2-Propanol, formic acid, were purchased from Thermo Fisher Scientific (Waltham, USA). Chloroform was obtained from Titan Technology Co. Ltd. (Shanghai, China).

Standards, such as ACC (SIGMA, 22059-21-8), ABA (Yuanye, 14375-45-2), SA (Yuanye, 69-72-7), and JA (SIGMA, 77026-92-7), were purchased from SIGMA and Yuanye, respectively. Stock solutions of a single standard were prepared at 1 mg/mL in MeOH. Primary mixed standard stock solution (MSS) was prepared by mixing the single standard stock solution, and diluting it with MeOH-water (5:95, v/v) to appropriate concentrations. Calibration curves were obtained by diluting the MSS with MeOH-water (5:95, v/v) to a concentration gradient.

Liquid chromatography was performed on a Nexera UHPLC LC-30A (SHIMADZU). An ACQUITY UPLC HSS T3 system, equipped with an electrospray ionisation (ESI) source, was applied for analysis. Targeted hormones were determined in a multiple reaction monitoring (MRM) mode. Data acquisitions were conducted using Analyst software. The SCIEX OS-MQ software was applied to quantify all hormones.

5.4 | DNA Extraction and Internal Transcribed Spacer Region (ITS) Sequencing

Total DNAs were extracted from different sample groups ($N = 6$) by the CTAB method (Kumar et al. 2024). The purified DNAs were PCR amplified with primers ITS1 (5′-GTGAR TCATCGAATCTTTG-3′) and ITS2 (5′-TCCTCCGCTTATTGA TATGC-3′) on the NovaSeq PE250 platform following its instructions. High-quality tag sequences without the barcodes and primers were obtained using the Fqtrim software (ver. 0.9.7). Chimeric sequences were filtered using Vsearch software (ver. 2.3.4) and were dereplicated using the DADA2 package (ver. 1.8). Alpha and beta diversities were calculated by QIIME2

with R (ver. 3.5.2), and the relative abundance was used to determine fungi taxonomy.

5.5 | ITS Sequence Data Analysis

Alpha diversity was calculated by Chao, Simpson and Shannon index based on the normalised counts using the vegan ver. 2.5.6R package (https://www.r-project.org/). The beta diversity was calculated by principal coordinates analysis, using Bray-Curtis dissimilarity and visualised using ggplot2 packages. A one-way analysis of similarity was applied to evaluate the effects of twig age on the endophytic fungus communities and secondary metabolism ($p < 0.05$). The LEfSe ($p < 0.05$) was used to analyse the effect of twig age on the relative abundance of fungal taxa from genera to species.

5.6 | RNA-Sequencing and Transcriptomic Data Analysis

Total RNAs were extracted using an Qiagen RNeasy Mini Kit (Hilden, Germany). The purified and fragmented mRNAs were used to construct cDNA libraries using a VAHTS Universal V6 RNA-seq Library Prep Kit. RNA sequencing was carried out on an Illumina 6000 platform (OEbiotech, Shanghai, China) to produce raw sequences (Feng et al. 2023).

Raw reads in fastq format were processed using the fastp programme, and the low quality reads were deleted to produce clean reads. The clean reads were mapped onto the *T. mairei* genome using HIST2 software. The read counts of each gene were calculated by HTSeq-count software. PCA was performed using R (ver. 3.2.0) to evaluate the sample supplication. DEGs were screened using the DESeq. 2 software based on a threshold of $p < 0.05$ and foldchange > 2 or < 0.5. Hierarchical cluster analysis of DEGs was performed using R (ver. 3.2.0).

5.7 | Isolation and Characterisation of Endophytic Fungal Isolates

Fresh twigs of *T. mairei* were surface washed and sterilised by immersion in 75% ethanol and 1.5% sodium hypochlorite twice. The resulting samples were cut into small pieces and kept on PDA solid medium with 30 μg/mL streptomycin sulphate. The emerging fungi were harvested and transferred to fresh PDA medium to obtain pure cultures.

The genomic DNA of each endophytic fungal isolates was extracted by the CTAB method. The ITS region of genomic DNA were amplified using ITS1FI2 (5′-GTGARTCATCG AATCTTTG-3′) and ITS2 (5′-TCCTCCGCTTATTGATATG C-3′) primers. The PCR products were sequenced and searched against the NCBI GenBank database. The endophytic fungi isolates were characterised based on three parameters, including identity, maximum query, and score.

5.8 | Inoculation of Endophytic Fungi With *T. mairei* Twigs

For metabolomic analysis, all eleven selected endophytic fungi (J02, J10, R01, L01, L13, M5, M8, M11, N13, N16, and N42) were incubated on Potato Dextrose Agar (PDA) for 7 days to produce spores. Spores with a uniform concentration were used for inoculation assays. The surface washed twigs were sprayed with 1 mL of spore suspension of each endophytic fungus. The concentration of the spore suspension was adjusted to 1×10^6 spores/mL, and ddH_2O was used as the negative control. After 48 h incubation, the twigs of *T. mairei* were harvested and washed with ddH_2O for untargeted metabolomic analysis.

For transcriptomic analysis, two selected endophytic fungi (L01 and J02) were incubated on Potato Dextrose Agar (PDA) for 7 days to produce spores. The concentration of the spore suspension was adjusted to 1×10^6 spores/mL, and ddH_2O was used as the negative control. After 48 h incubation, the treated area of each twig was washed with ddH_2O twice and harvested for transcriptomic analysis.

5.9 | Promoter and Gene Sequence Analysis

The promoter sequences of several selected genes were extracted from the public *T. mairei* genome. The 2000 bp promoter regions were scanned using the PlantCARE programme for several typical MYC binding elements. Phylogenetic tree was constructed using MEGA 7.1 software and the CLUSTALW programme employing the Neighbour-Joining method (Saitou and Nei 1987).

5.10 | Prokaryotic Expression and Electrophoretic Mobility Shift Assay

The full-length CDS of *MYC2a* was cloned and inserted into pGEX-6P-1 vector and prokaryotic expressed in *Escherichia coli* cells to produce recombinant GST-MYC2a protein. The expressed protein was purified using Clontech His60 Ni Superflow Resin and EMSA was performed using the Light Shift Chemiluminescent EMSA Kit (GS009, Beyotime, China). Briefly, probes containing MYC2-specific *cis*-elements (CAAATGC, CACATG, CATTTG, and CATGTG) derived from the promoters of seven Taxol biosynthesis-related genes were labelled with 506-FAM (FITC) fluorescent dye. The probes were incubated with the nuclear extract at room temperature for 30 min. The entire reaction mixture was run on a non-denaturing 0.5 × TBE 6% polyacrylamide gel for 1 h at 60 V at 4°C and then transferred onto Biodyne B nylon membranes (Pall Corporation). Signals were visualised with reagents included in the kit and ChemiDoc XRS (Bio-Rad Laboratories, UAS). Unlabelled probes were used in competition assays. MYC2-specific *cis*-elements within probes were changed into CCCCCC and used in mutation assays.

5.11 | Dual-LUC Reporter Assays

The full-length CDS of *MYC2a* gene was cloned into the pGreenII62-SK vector to build effector, and the promoters of

DBTNBT (ctg195_gene.25), *T7OH* (ctg2120_gene.17), *TS* (ctg5306_gene.4), *T13OH* (ctg593_gene.12), and *TS* (ctg7747_gene.1) were cloned into pGreenII0800-LUC vector to build reporters. The GAL4BD and VP16 were prepared as positive and negative controls, respectively. All completed constructs were co-transformed into tobacco (*Nicotiana tabacum*) leaves by Agrobacterium tumefaciens GV3101-mediated transient expression. The firefly LUC and Renilla luciferase activities were determined using a dual-LUC assay kit (Promega, Madison, USA). All primers and probes are listed in Table S8.

Acknowledgements

We are grateful to LC Sciences company (Hangzhou, China) and OE-biotech Co. Ltd (Shanghai, China) for transcriptomic and metabolomic analysis, respectively. This work was funded by the National Natural Science Foundation of China (Grant Nos. 32271905 and 32270382), the Zhejiang Provincial Natural Science Foundation of China (Grant Nos. LY23C160001 and LY22C020001), and Hangzhou Joint Fund of the Zhejiang Provincial Natural Science Foundation of China (Grant No. LHZY24C140001).

Conflicts of Interest

The authors declare no conflicts of interest.

Data Availability Statement

The raw transcriptome sequencing data are uploaded to the National Center for Biotechnology Information under BioProject ID: GSE263216. The raw metabolome data are uploaded to OMIX database under BioProject ID: PRJCA024086 and the data accessibility is Open-access, see OMIX005959. The *T. mairei* reference genome was downloaded from the NCBI database (ID: PRJNA730337).

References

Adamczyk, S., S. Latvala, A. Poimala, B. Adamczyk, T. Hytönen, and T. Pennanen. 2023. "Diterpenes and Triterpenes Show Potential as Biocides Against Pathogenic Fungi and Oomycetes: A Screening Study." *Biotechnology Letters* 45, no. 11–12: 1555–1563. https://doi.org/10.1007/s10529-023-03438-z.

Beilsmith, K., M. Perisin, and J. Bergelson. 2021. "Natural Bacterial Assemblages in *Arabidopsis thaliana* Tissues Become More Distinguishable and Diverse During Host Development." *mBio* 12, no. 1: e02723-20. https://doi.org/10.1128/mBio.02723-20.

Cao, X., L. Xu, L. Li, W. Wan, and J. Jiang. 2022. "TcMYB29a, an ABA-Responsive R2R3-MYB Transcriptional Factor, Upregulates Taxol Biosynthesis in Taxus chinensis." *Frontiers in Plant Science* 13: 804593. https://doi.org/10.3389/fpls.2022.804593.

Cao, X., L. Xu, J. Wang, et al. 2022. "Endophytic Fungus Pseudodidymocyrtis lobariellae KL27 Promotes Taxol Biosynthesis and Accumulation in Taxus chinensis." *BMC Plant Biology* 22, no. 1: 12. https://doi.org/10.1186/s12870-021-03396-6.

Chen, D., Y. Wang, W. Shi, et al. 2022. "Analysis of Endophyte Diversity of *Rheum palmatum* Among Different Tissues and Ages." *Archives of Microbiology* 205, no. 1: 14. https://doi.org/10.1007/s00203-022-03349-z.

Chen, Y., H. Zhang, M. Zhang, et al. 2021. "Salicylic Acid-Responsive Factor TcWRKY33 Positively Regulates Taxol Biosynthesis in Taxus Chinensis in Direct and Indirect Ways." *Frontiers in Plant Science* 12: 697476. https://doi.org/10.3389/fpls.2021.697476.

Cheng, T., M. Kolařík, L. Quijada, and M. Stadler. 2022. "A Re-Assessment of Taxomyces Andreanae, the Alleged Taxol-Producing Fungus, Using Comparative Genomics." *IMA Fungus* 13, no. 1: 17. https://doi.org/10.1186/s43008-022-00103-4.

Cui, Y., R. Mao, J. Chen, and Z. Guo. 2019. "Regulation Mechanism of MYC Family Transcription Factors in Jasmonic Acid Signalling Pathway on Taxol Biosynthesis." *International Journal of Molecular Sciences* 20, no. 8: 1843. https://doi.org/10.3390/ijms20081843.

Demidova, E., E. Globa, A. Klushin, D. Kochkin, and A. Nosov. 2023. "Effect of Methyl Jasmonate on the Growth and Biosynthesis of C13- and C14-Hydroxylated Taxoids in the Cell Culture of Yew (Taxus wallichiana Zucc.) of Different Ages." *Biomolecules* 13, no. 6: 969. https://doi.org/10.3390/biom13060969.

Escrich, A., L. Almagro, E. Moyano, et al. 2021. "Improved Biotechnological Production of Paclitaxel in *Taxus media* Cell Cultures by the Combined Action of Coronatine and calix[8]arenes." *Plant Physiology and Biochemistry* 163: 68–75. https://doi.org/10.1016/j.plaphy.2021.03.047.

Exposito, O., M. Bonfill, E. Moyano, et al. 2009. "Biotechnological Production of Taxol and Related Taxoids: Current State and Prospects." *Anti-Cancer Agents in Medicinal Chemistry* 9, no. 1: 109–121. https://doi.org/10.2174/187152009787047761.

Fan, M., X. Chen, X. Luo, et al. 2020. "Diversity of Endophytic Fungi From the Leaves of Vaccinium dunalianum." *Letters in Applied Microbiology* 71, no. 5: 479–489. https://doi.org/10.1111/lam.13345.

Feng, S., K. Hou, H. Zhang, et al. 2023. "Investigation of the Role of TmMYB16/123 and Their Targets (TmMTP1/11) in the Tolerance of *Taxus media* to Cadmium." *Tree Physiology* 43: 1009–1022. https://doi.org/10.1093/treephys/tpad019.

Fu, Y., X. Li, X. Yuan, et al. 2023. "*Alternaria alternata* F3, a Novel Taxol-Producing Endophytic Fungus Isolated From the Fruits of *Taxus Cuspidata*: Isolation, Characterization, Taxol Yield Improvement, and Antitumor Activity." *Applied Biochemistry and Biotechnology* 196: 2246–2269. https://doi.org/10.1007/s12010-023-04661-0.

Gallego, A., N. Imseng, M. Bonfill, et al. 2015. "Development of a Hazel Cell Culture-Based Paclitaxel and Baccatin III Production Process on a Benchtop Scale." *Journal of Biotechnology* 195: 93–102. https://doi.org/10.1016/j.jbiotec.2014.12.023.

Ibrahim, D., C. C. Lee, and L. Sheh-Hong. 2014. "Antimicrobial Activity of Endophytic Fungi Isolated From *Swietenia macrophylla* Leaves." *Natural Product Communications* 9, no. 2: 247–250.

Kaspera, R., and R. Croteau. 2006. "Cytochrome P450 Oxygenases of Taxol Biosynthesis." *Phytochemistry Reviews* 5, no. 2–3: 433–444. https://doi.org/10.1007/s11101-006-9006-4.

Kumar, A., J. Singh, D. Panwar, et al. 2024. "An Improved DNA Extraction Method in Okra for Rapid PCR Detection of Okra Enation Leaf Curl Virus From Diverse Indian Regions." *Archives of Microbiology* 206, no. 12: 468. https://doi.org/10.1007/s00203-024-04176-0.

Kumar, A., S. Singh, and A. Pandey. 2009. "General Microflora, Arbuscular Mycorrhizal Colonization and Occurrence of Endophytes in the Rhizosphere of Two Age Groups of *Ginkgo biloba* L. of Indian Central Himalaya." *Indian Journal of Microbiology* 49, no. 2: 134–141. https://doi.org/10.1007/s12088-009-0017-x.

Latz, M. A. C., M. H. Kerrn, H. Sørensen, et al. 2021. "Succession of the Fungal Endophytic Microbiome of Wheat Is Dependent on Tissue-Specific Interactions Between Host Genotype and Environment." *Science of the Total Environment* 759: 143804. https://doi.org/10.1016/j.scitotenv.2020.143804.

Li, C., Y. Qi, Z. Sun, M. Jiang, and C. Li. 2023. "Way to Efficient Microbial Paclitaxel Mass Production." *Synthetic and Systems Biotechnology* 8, no. 4: 673–681. https://doi.org/10.1016/j.synbio.2023.10.002.

Li, Y., S. Li, R. Du, et al. 2021. "Isoleucine Enhances Plant Resistance Against Botrytis Cinerea via Jasmonate Signaling Pathway." *Frontiers in Plant Science* 12: 628328. https://doi.org/10.3389/fpls.2021.628328.

Liu, S., Y. Wang, M. Shi, et al. 2022. "SmbHLH60 and SmMYC2 Antagonistically Regulate Phenolic Acids and Anthocyanins

Biosynthesis in *Salvia miltiorrhiza*." *Journal of Advanced Research* 42: 205–219. https://doi.org/10.1016/j.jare.2022.02.005.

Liu, T., A. Greenslade, and S. Yang. 2017. "Levels of Rhizome Endophytic Fungi Fluctuate in Paris Polyphylla Var. Yunnanensis as Plants Age." *Plant Diversity* 39, no. 1: 60–64. https://doi.org/10.1016/j.pld.2016.11.006.

Machado, K. L. G., D. V. Faria, M. B. S. Duarte, et al. 2023. "Plant Age-Dependent Dynamics of Annatto Pigment (Bixin) Biosynthesis Inbixa Orellana." *Journal of Experimental Botany* 75: 1390–1406. https://doi.org/10.1093/jxb/erad458.

Masoudi Khorasani, F., A. Ganjeali, J. Asili, and M. Cheniany. 2023. "Beneficial Effects of Endophytic Fungi Inoculation on Tanshinones and Phenolic Compounds of Salvia Abrotanoides." *Iranian Journal of Basic Medical Sciences* 26, no. 4: 408–413. https://doi.org/10.22038/ijbms.2023.67730.14828.

Miao, L. Y., X. C. Mo, X. Y. Xi, et al. 2018. "Transcriptome Analysis of a Taxol-Producing Endophytic Fungus *Cladosporium cladosporioides* MD2." *AMB Express* 8, no. 1: 41. https://doi.org/10.1186/s13568-018-0567-6.

Osono, T. 2008. "Endophytic and Epiphytic Phyllosphere Fungi of *Camellia japonica*: Seasonal and Leaf Age-Dependent Variations." *Mycologia* 100, no. 3: 387–391. https://doi.org/10.3852/07-110r1.

Qiao, W., T. Tang, and F. Ling. 2020. "Comparative Transcriptome Analysis of a Taxol-Producing Endophytic Fungus, *Aspergillus aculeatinus* Tax-6, and Its Mutant Strain." *Scientific Reports* 10, no. 1: 10558. https://doi.org/10.1038/s41598-020-67614-1.

Saitou, N., and M. Nei. 1987. "The Neighbor-Joining Method: A New Method for Reconstructing Phylogenetic Trees." *Molecular Biology and Evolution* 4, no. 4: 406–425. https://doi.org/10.1093/oxfordjournals.molbev.a040454.

Salehi, M., S. Farhadi, A. Moieni, N. Safaie, and M. Hesami. 2021. "A Hybrid Model Based on General Regression Neural Network and Fruit Fly Optimization Algorithm for Forecasting and Optimizing Paclitaxel Biosynthesis in *Corylus avellana* Cell Culture." *Plant Methods* 17, no. 1: 13. https://doi.org/10.1186/s13007-021-00714-9.

Salehi, M., A. Moieni, N. Safaie, and S. Farhadi. 2020. "Whole Fungal Elicitors Boost Paclitaxel Biosynthesis Induction in *Corylus avellana* Cell Culture." *PLoS One* 15, no. 7: e0236191. https://doi.org/10.1371/journal.pone.0236191.

Sng, B. J. R., B. Mun, B. Mohanty, et al. 2021. "Combination of Red and Blue Light Induces Anthocyanin and Other Secondary Metabolite Biosynthesis Pathways in an Age-Dependent Manner in Batavia Lettuce." *Plant Science* 310: 110977. https://doi.org/10.1016/j.plantsci.2021.110977.

Sykłowska-Baranek, K., G. Sygitowicz, A. Maciejak-Jastrzębska, A. Pietrosiuk, and A. Szakiel. 2022. "Application of Priming Strategy for Enhanced Paclitaxel Biosynthesis in Taxus × Media Hairy Root Cultures." *Cells* 11, no. 13: 2062. https://doi.org/10.3390/cells11132062.

Toghueo, R. M. K., I. Zabalgogeazcoa, E. C. Pereira, and B. R. Vazquez de Aldana. 2022. "A Diaporthe Fungal Endophyte From a Wild Grass Improves Growth and Salinity Tolerance of Tritordeum and Perennial Ryegrass." *Frontiers in Plant Science* 13: 896755. https://doi.org/10.3389/fpls.2022.896755.

Wang, B., C. Chen, Y. Xiao, et al. 2023. "Geographically Associated Endophytic Fungi Contribute to the Tropane Alkaloids Accumulation of *Anisodus tanguticus*." *Frontiers in Plant Science* 14: 1297546. https://doi.org/10.3389/fpls.2023.1297546.

Wang, C., J. Wu, and X. Mei. 2001. "Enhancement of Taxol Production and Excretion in Taxus Chinensis Cell Culture by Fungal Elicitation and Medium Renewal." *Applied Microbiology and Biotechnology* 55, no. 4: 404–410. https://doi.org/10.1007/s002530000567.

Wani, M. C., and S. B. Horwitz. 2014. "Nature as a Remarkable Chemist: A Personal Story of the Discovery and Development of Taxol." *Anti-Cancer Drugs* 25, no. 5: 482–487. https://doi.org/10.1097/cad.0000000000000063.

Wu, L. S., W. G. Dong, J. P. Si, J. J. Liu, and Y. Q. Zhu. 2020. "Endophytic Fungi, Host Genotype, and Their Interaction Influence the Growth and Production of Key Chemical Components of *Dendrobium catenatum*." *Fungal Biology* 124, no. 10: 864–876.

Wu, Z., Q. Su, Y. Cui, et al. 2020. "Temporal and Spatial Pattern of Endophytic Fungi Diversity of *Camellia sinensis* (cv. Shu Cha Zao)." *BMC Microbiology* 20, no. 1: 270. https://doi.org/10.1186/s12866-020-01941-1.

Xiong, Z. Q., Y. Y. Yang, N. Zhao, and Y. Wang. 2013. "Diversity of Endophytic Fungi and Screening of Fungal Paclitaxel Producer From Anglojap yew, *Taxus* x *media*." *BMC Microbiology* 13: 71. https://doi.org/10.1186/1471-2180-13-71.

Xue, B., J. Zhao, Y. Fan, et al. 2020. "Synthesis of Taxol and Docetaxel by Using 10-Deacetyl-7-Xylosyltaxanes." *Chemistry & Biodiversity* 17, no. 2: e1900631. https://doi.org/10.1002/cbdv.201900631.

Yan, L., J. Zhu, X. Zhao, J. Shi, C. Jiang, and D. Shao. 2019. "Beneficial Effects of Endophytic Fungi Colonization on Plants." *Applied Microbiology and Biotechnology* 103, no. 8: 3327–3340. https://doi.org/10.1007/s00253-019-09713-2.

Ye, H. T., S. Q. Luo, Z. N. Yang, et al. 2021. "Endophytic Fungi Stimulate the Concentration of Medicinal Secondary Metabolites in *Houttuynia cordata* Thunb." *Plant Signaling & Behavior* 16, no. 9: 1929731. https://doi.org/10.1080/15592324.2021.1929731.

Yu, C., K. Hou, H. Zhang, et al. 2023. "Integrated Mass Spectrometry Imaging and Single-Cell Transcriptome Atlas Strategies Provide Novel Insights Into Taxoid Biosynthesis and Transport in *Taxus mairei* Stems." *Plant Journal* 115: 1243–1260. https://doi.org/10.1111/tpj.16315.

Yu, C., J. Huang, Q. Wu, et al. 2022. "Role of Female-Predominant MYB39-bHLH13 Complex in Sexually Dimorphic Accumulation of Taxol in *Taxus media*." *Horticulture Research* 9: uhac062. https://doi.org/10.1093/hr/uhac062.

Yu, C., X. Luo, X. Zhan, et al. 2018. "Comparative Metabolomics Reveals the Metabolic Variations Between Two Endangered Taxus Species (*T. fuana* and *T. yunnanensis*) in the Himalayas." *BMC Plant Biology* 18, no. 1: 197. https://doi.org/10.1186/s12870-018-1412-4.

Yu, C., X. Zhan, C. Zhang, et al. 2021. "Comparative Metabolomic Analyses Revealed the Differential Accumulation of Taxoids, Flavonoids and Hormones Among Six Taxaceae Trees." *Scientia Horticulturae* 285: 110196. https://doi.org/10.1016/j.scienta.2021.110196.

Zhan, X., T. Qiu, H. Zhang, et al. 2023. "Mass Spectrometry Imaging and Single-Cell Transcriptional Profiling Reveal the Tissue-Specific Regulation of Bioactive Ingredient Biosynthesis in Taxus Leaves." *Plant Communications* 4: 100630. https://doi.org/10.1016/j.xplc.2023.100630.

Zhan, X., H. Zhang, X. Liang, et al. 2023. "Single-Cell ATAC Sequencing Illuminates the Cis-Regulatory Differentiation of Taxol Biosynthesis Between Leaf Mesophyll and Leaf Epidermal Cells in *Taxus mairei*." *Industrial Crops and Products* 205: 117411. https://doi.org/10.1016/j.indcrop.2023.117411.

Zhang, H., K. Hou, X. Liang, et al. 2024. "Sex-Specific Responses of *Taxus mairei* to UV-B Radiation Involved Altering the Interactions Between the Microbiota Assembly and Host Secondary Metabolism." *Microbiome* 12, no. 1: 165. https://doi.org/10.1186/s40168-024-01882-1.

Zhang, H., W. Lin, R. Ma, et al. 2024. "Fungal Endophytes of *Taxus* Species and Regulatory Effect of Two Strains on Taxol Synthesis." *BMC Microbiology* 24, no. 1: 291. https://doi.org/10.1186/s12866-024-03445-8.

Zhang, M., X. Jin, Y. Chen, et al. 2018. "TcMYC2a, a Basic Helix-Loop-Helix Transcription Factor, Transduces JA-Signals and Regulates Taxol Biosynthesis in *Taxus chinensis*." *Frontiers in Plant Science* 9: 863. https://doi.org/10.3389/fpls.2018.00863.

Zhang, S., T. Ye, Y. Liu, et al. 2023. "Research Advances in Clinical Applications, Anticancer Mechanism, Total Chemical Synthesis,

Semi-Synthesis and Biosynthesis of Paclitaxel." *Molecules* 28, no. 22: 7517. https://doi.org/10.3390/molecules28227517.

Zhao, Z., Y. Zhang, W. Li, Y. Tang, and S. Wang. 2023. "Transcriptomics and Physiological Analyses Reveal Changes in Paclitaxel Production and Physiological Properties in *Taxus cuspidata* Suspension Cells in Response to Elicitors." *Plants* 12, no. 22: 3817. https://doi.org/10.3390/plants12223817.

Zheng, M., S. Zhong, W. Wang, Z. Tang, T. Bu, and Q. Li. 2023. "*Serendipita indica* Promotes the Growth of Tartary Buckwheat by Stimulating Hormone Synthesis, Metabolite Production, and Increasing Systemic Resistance." *Journal of Fungi* 9, no. 11: 1114. https://doi.org/10.3390/jof9111114.

Supporting Information

Additional supporting information can be found online in the Supporting Information section.